Neuron
Article

# Molecular Motor KIF5A Is Essential for $GABA_A$ Receptor Transport, and KIF5A Deletion Causes Epilepsy

Kazuo Nakajima,[1] Xiling Yin,[1] Yosuke Takei,[1] Dae-Hyun Seog,[3] Noriko Homma,[1] and Nobutaka Hirokawa[1,2,*]
[1]Department of Cell Biology and Anatomy, Graduate School of Medicine, The University of Tokyo, Hongo, Tokyo 113-0033, Japan
[2]Center of Excellence in Genomic Medicine Research, King Abdulaziz University, Jeddah 21589, Saudi Arabia
[3]Department of Biochemistry, College of Medicine, Inje University, Busan 614-735, Korea
*Correspondence: hirokawa@m.u-tokyo.ac.jp
http://dx.doi.org/10.1016/j.neuron.2012.10.012

## SUMMARY

**KIF5 (also known as kinesin-1) family members, consisting of KIF5A, KIF5B, and KIF5C, are microtubule-dependent molecular motors that are important for neuronal function. Among the KIF5s, KIF5A is neuron specific and highly expressed in the central nervous system. However, the specific roles of KIF5A remain unknown. Here, we established conditional *Kif5a*-knockout mice in which KIF5A protein expression was postnatally suppressed in neurons. Epileptic phenotypes were observed by electroencephalogram abnormalities in knockout mice because of impaired $GABA_A$ receptor ($GABA_AR$)-mediated synaptic transmission. We also identified reduced cell surface expression of $GABA_AR$ in knockout neurons. Importantly, we identified that KIF5A specifically interacted with $GABA_AR$-associated protein (GABARAP) that is known to be involved in $GABA_AR$ trafficking. KIF5A regulated neuronal surface expression of $GABA_ARs$ via an interaction with GABARAP. These results provide an insight into the molecular mechanisms of KIF5A, which regulate inhibitory neural transmission.**

## INTRODUCTION

Kinesin superfamily proteins (KIFs) are microtubule-dependent molecular motors for intracellular transport and have been reported to transport various types of cargo, including organelles, synaptic vesicle precursors, neurotransmitter receptors, cell signaling molecules, cell adhesion molecules, and mRNAs, in the neurons of mammalian nervous systems (Hirokawa and Noda, 2008; Schliwa, 2002). Thus, KIFs are one of the important molecular components that manage fundamental neuronal functions, such as viability, morphogenesis, and plasticity, as well as the pathogenesis of neurological disorders (Hirokawa et al., 2010).

KIF5s, also known as kinesin-1 family members (Lawrence et al., 2004; Miki et al., 2005), consist of KIF5A, KIF5B, and KIF5C, each of which is encoded by a different gene and possess a similar motor domain containing an ATP-binding motif at the N terminus and a different cargo-binding domain (BD) at the C terminus. Several studies have reported the functions of KIF5A, KIF5B, and KIF5C. *Kif5b*-knockout (KO) mice are embryonic lethal and show abnormal localization of mitochondria in their extraembryonic cells (Tanaka et al., 1998). *Kif5c*-KO mice are normal in their appearance but show a smaller brain size and relative loss of motor neurons compared with sensory neurons (Kanai et al., 2000). *Kif5a*-KO mice are neonatal lethal but show no apparent histological abnormalities in their brains except that the nuclei and cell bodies of spinal cord motor neurons appear to be larger than the wild-type (WT) (Xia et al., 2003). More than 75% of conditional *Kif5a*-KO mice die within 3 weeks and undergo seizures, whereas the remaining mice survive for up to 3 months or even longer and show abnormal neurofilament (NF) accumulation (Xia et al., 2003). Although this study describes various phenotypes caused by the absence of KIF5A, there has been no explanation for the premature death and seizures caused by postnatal loss of KIF5A (Hirokawa and Takeda, 1998; Lariviere and Julien, 2004). In addition, although numerous types of cargoes common to KIF5A, KIF5B, and KIF5C have been reported, KIF5A-specific cargo has not been reported. Thus, we searched for KIF5A-specific binding partners and examined its relationships with the phenotypes of *Kif5a*-KO mice.

## RESULTS

### Electroencephalographic Recording Identifies Spontaneous Epileptic Seizure and Impaired Neuronal Network Activity Caused by Postnatal Loss of KIF5A

We generated conditional *Kif5a*-KO ($Kif5a^{-/-}$) mice using the Cre/*loxP* gene-targeting strategy (Figures S1A–S1C available online). Immunoblotting of whole-brain lysates using an anti-KIF5A polyclonal antibody confirmed the complete absence of KIF5A in the $Kif5a^{-/-}$ mouse (Figure S1D). These $Kif5a^{-/-}$ mice died shortly after birth. To circumvent lethality and postnatally analyze the gene function of *Kif5a*, we used a rat synapsin promoter-driven Cre transgenic line ($Syn\text{-}Cre^{tg/\bullet}$) (Zhu et al., 2001) and crossed $Kif5a^{+/-};Syn\text{-}Cre^{tg/\bullet}$ mice with $Kif5a^{fl/fl}$ mice to obtain conditional KO mice ($Kif5a^{fl/-};Syn\text{-}Cre^{tg/\bullet}$). We considered the other three genotypes of mice ($Kif5a^{fl/+}$, $Kif5a^{fl/+};Syn\text{-}Cre^{tg/\bullet}$, and $Kif5a^{fl/-}$) as controls because their general

appearance and body sizes were normal. In addition, we did not find any structural abnormalities in their brains or observe behavioral abnormalities. Postnatal growth of *Kif5a*-conditional KO mice was indistinguishable from that of control mice for up to 1 week. However, after the first week, conditional *Kif5a*-KO mice showed growth retardation and died at approximately 3 weeks postnatally. We did not find any *Kif5a*-conditional KO mice that survived for 4 weeks after birth in all litters used in this study (more than 50 litters). Immunoblotting of whole-brain lysates showed that KIF5A protein expression levels in *Kif5a*-conditional KO mouse brains ranged from 14% to 47% of those in control mouse brains (Figure 1A). There were no apparent histological abnormalities in the brains of *Kif5a*-KO and conditional KO mice (Figures S1E and S1F).

Although postnatal loss of KIF5A has been reported to cause seizures (Xia et al., 2003), the observation was limited to the general appearance of mice. In this study, we performed electroencephalographic (EEG) recording of control and *Kif5a*-conditional KO mice. The electrode was implanted into the hippocampus of the brain (Figures 1B–1H). In the *Kif5a*-conditional KO mouse brain, paroxysmal sharp waves were often observed in rest and locomotive states (Figures 1F and 1G; Movies S1 and S2). Long-term recording during night periods identified repetitive spike-wave discharges that are known to represent a classical epileptic EEG (McCormick and Contreras, 2001) (Figure 1H). After these epileptic seizure events, *Kif5a*-conditional KO mice occasionally did not recover normal leg movement for up to 2 hr (Figure 1I; Movie S3). A small number of mice repeated this epileptic episode several times during the night. To analyze the baseline EEG (Figures 1B–1E), we performed a power analysis by fast Fourier transform (Otnes, 1978) of raw EEG data (Figures 1J and 1K). The profile of EEG power of *Kif5a*-conditional KO mice showed a significant power reduction in both rest and locomotive states, suggesting that neuronal network activity is impaired by postnatal loss of KIF5A. All procedures were approved by the Graduate School of Medicine, The University of Tokyo.

## Loss of KIF5A Causes an Impairment of $GABA_A$R-Mediated Neurotransmission in the Hippocampus

Because it is known that disturbance of inhibitory synaptic transmission is involved in epileptic seizure generation (Jacob et al., 2008; Rudolph and Möhler, 2004), we speculated that GABAergic synaptic transmission may be impaired in the hippocampus of *Kif5a*-conditional KO mice. We performed whole-cell patch-clamp recordings to investigate the miniature inhibitory postsynaptic currents (mIPSCs) in the CA1 region of hippocampal slices (Figure 2A). We observed a significantly reduced mean amplitude of mIPSCs in the slices of *Kif5a*-conditional KO mice compared with those of controls (control, 16.5 ± 0.7 pA; conditional KO, 8.5 ± 0.4 pA). A cumulative probability curve also indicated a leftward shift to smaller amplitudes in *Kif5a*-conditional KO mice (Figure 2F). However, the frequency, rise time, and decay time, although slightly reduced, were not statistically different between genotypes (Figures 2C–2E and 2G). Furthermore, the ratio of evoked (e)IPSC (upward traces in Figure 2H) to 2-amino-3-(5-methyl-3-oxo-1, 2-oxazol-4-yl) propanoic acid (AMPA)-mediated evoked EPSC (downward traces in Figure 2H) was reduced in *Kif5a*-conditional KO mouse slices, compared with that in control mouse slices (Figure 2H), showing a relative reduction in eIPSC amplitudes in *Kif5a*-KO neurons. Taken together, these results suggest that $GABA_A$ receptor ($GABA_A$R)-mediated synaptic transmission is impaired in the hippocampus of *Kif5a*-conditional KO mice. Next, to investigate network excitability, we measured stimulus-evoked population spikes in hippocampal slices of *Kif5a*-conditional KO and control slices. Epileptiform activities were more frequently observed in *Kif5a*-conditional KO slices in both standard and $Mg^{2+}$-depleted artificial cerebrospinal fluid (ACSF), indicating increased excitability in these tissues (Figures 2J–2O).

To investigate the cause of impairment in inhibitory synaptic transmission, we compared cell surface expression of $GABA_A$Rs in primary hippocampal neurons derived from *Kif5a*-KO and WT embryos. Most $GABA_A$Rs at synapses are thought to be composed of two α1, α2, or α3 subunits together with two β2 or β3 subunits and a single γ2 subunit. Using the surface biotinylation method, the cell surface expression level of $GABA_A$Rβ2 was assessed. In KO neurons, cell surface expression of $GABA_A$Rβ2 was significantly reduced (52.6% ± 4.9% versus WT), whereas that of GluR2/3 was unchanged (Figures 3A and 3B). Immunofluorescence staining of cell surface $GABA_A$Rβ2/3 revealed that the cell surface receptor density was significantly reduced in KO cells (15.6 ± 2.1 versus 28.5 ± 2.0 in WT) (Figures 3C and 3D). We further investigated the amount of $GABA_A$Rs in the intracellular fraction by immunoprecipitation using the remaining cell lysate after the cell surface fraction was removed by the surface biotinylation method. In *Kif5a*-KO neurons, the amount of $GABA_A$Rβ2 probed with an anti-$GABA_A$Rβ2 antibody was increased compared with that of the WT (Figures 3E and 3F), suggesting that a larger amount of $GABA_A$Rβ2 protein was retained in the cytoplasm of *Kif5a*-KO neurons. To assess the possible alteration of endocytotic dynamics in KO neurons, we performed an endocytosis assay of $GABA_A$Rs. The fluorescent signal of endocytosed $GABA_A$Rβ2/3 was not significantly different between WT and *Kif5a*-KO neurons (Figures 3G and 3H). These results suggest that the reduced cell surface expression of $GABA_A$Rs in KO neurons is caused by impaired trafficking of $GABA_A$Rs from the intracellular pool to the cell surface, and not by accelerated removal of $GABA_A$Rs from the cell surface. On the other hand, immunoblotting showed that the total expression level of $GABA_A$Rs did not significantly change in KO (Figure 3I) and *Kif5a*-conditional KO brain lysates (Figure 3J). Together, these data suggest that ablation of KIF5A does not affect overall expression of $GABA_A$Rs but alters the subcellular localization of $GABA_A$Rs. The abnormal localization of $GABA_A$Rs observed in *Kif5a*-KO neurons raised the possibility that KIF5A has a specific role in the trafficking of $GABA_A$Rs among KIF5 members (KIF5A/KIF5B/KIF5C).

To test this possibility, we conducted rescue experiments (Figures 3K and 3L). We transfected *Kif5a*-KO neurons with a full-length KIF5A, KIF5B, or KIF5C construct. Neurons transfected with KIF5A recovered cell surface expression of $GABA_A$Rs; number of puncta/50 μm dendrite (WT, 13.6 ± 0.5; KO, 6.4 ± 0.3; KO + KIF5A, rescued, 11.8 ± 0.4) (mean ± SEM, n = 15 neurons from three mice). However, neurons transfected

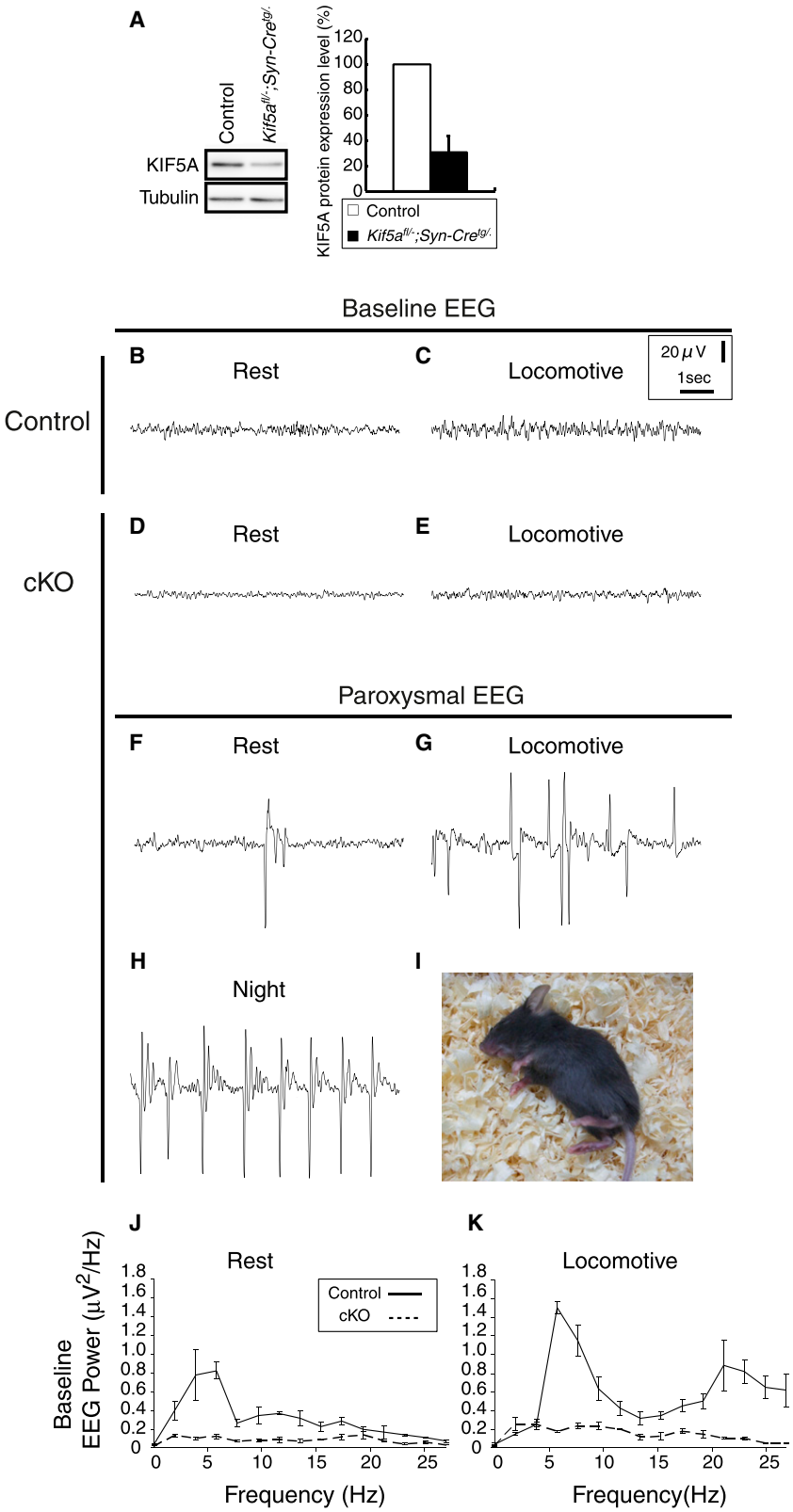


**Figure 1. Abnormal EEG of *Kif5a*-Conditional KO Mouse Brain**

(A) Left view is an immunoblot showing a significant loss of KIF5A protein in the whole-brain lysate of a conditional KO mouse (postnatal day 14). In this immunoblot, a 70% decrease of KIF5A protein expression was observed, compared with that of the control. Tubulin was used as a loading control. Right view shows statistics of KIF5A protein expression levels (normalized to tubulin expression, n = 5 independent experiments; **p < 0.001, Welch's t test). Error bar represents mean ± SD. EEG recordings were obtained from three mice for each genotype, and representative waveforms are shown.

(B–E) Baseline waveforms.

(F–H) Paroxysmal waveforms observed in conditional KO mice.

(I) Appearance of a conditional KO mouse that occasionally fell after repetitive epileptic spike-wave discharges as shown in (G) and could not recover for a few hours during the night.

(J and K) Power spectra obtained from fast Fourier analysis of the baseline EEG. Intervals of 4.5 s (for conditional KO, at least 10 s apart from paroxysmal EEG) were selected for each measurement and analysis. Three independent experiments, n = 3 mice for each frequency; Rest, p = 0.0037; Locomotive, p = 0.0011; Repeated-measure ANOVA. Error bars represent mean ± SEM.

Related to Figure S1 and Movies S1, S2, and S3.

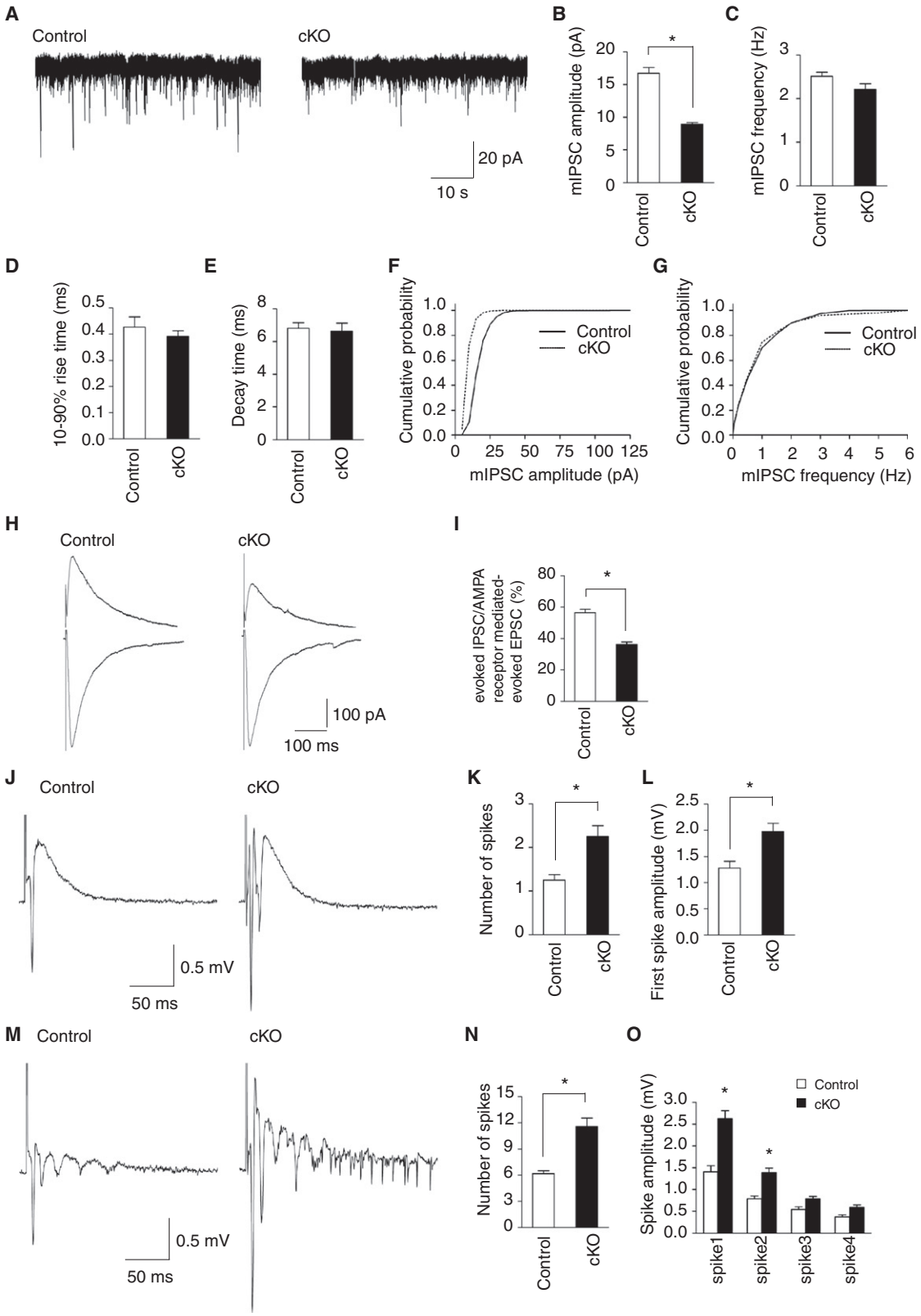


**Figure 2. GABA$_A$R-Mediated IPSCs and Stimulus-Evoked Population Spikes in Conditional *Kif5a*-KO Hippocampal Slices**

(A) Representative traces showing mIPSCs recorded from CA1 pyramidal cells of control and conditional *Kif5a*-KO (cKO) mice.

with KIF5B or KIF5C did not show a rescued phenotype. These data suggest that KIF5A is involved in $GABA_AR$ transport. Next, we performed knockdown of KIF5A, KIF5B, or KIF5C in neurons using miRNA vectors (Figures 3M and 3N). Specificity of the knockdown effect of each vector is shown in Figure S2. Knockdown of KIF5A specifically reduced the cell surface expression of $GABA_AR$s, whereas that of KIF5B or KIF5C did not; number of puncta/50 μm dendrite (nontransfected, 12.2 ± 0.5; miRNA for KIF5A, 6.1 ± 0.3; KIF5B, 10.5 ± 0.3; KIF5C, 12.1 ± 0.4) (mean ± SEM, n = 15 neurons from three mice). These results further suggest that KIF5A is a molecular motor involved in $GABA_AR$ trafficking in neurons and that this function of KIF5A is not compensated by KIF5B or KIF5C.

Because a previous report showed late-onset accumulation of NF proteins in the dorsal root ganglion sensory neurons of *Kif5a*-KO mice (Xia et al., 2003), we examined the level of NFs in *Kif5a*-KO mouse neurons. We did not find any significant increase of NF-H or NF-M protein expression or accumulation of dephosphorylated NF-H protein in *Kif5a*-KO neurons (Figures S3A and S3B). These results indicate that the observed $GABA_AR$ phenotypes are not due to an intracellular transport defect caused by impaired NF transport.

In addition, we performed immunocytochemistry of the Kv3.1b channel in hippocampal neurons because KIF5s are involved in axonal transport of the Kv3.1b channel by direct binding (Xu et al., 2010). The distribution of Kv3.1b was indistinguishable between genotypes in both axons and dendrites (Figures S4A and S4B).

## KIF5A Directly Interacts with $GABA_AR$-Associated Protein and Facilitates $GABA_AR$ Trafficking to the Neuronal Surface

Recently, KIF5s have been reported to interact with huntingtin-associated protein 1 (HAP1; known to be involved in $GABA_AR$ trafficking) via domains common to KIF5A, KIF5B, and KIF5C (Twelvetrees et al., 2010). However, among *Kif5a*-, *Kif5b*-, and *Kif5c*-KO mice (Kanai et al., 2000; Tanaka et al., 1998; Xia et al., 2003), only *Kif5a*-KO mice show phenotypes related to an impairment of $GABA_AR$ trafficking in neurons. *Kif5c*-KO mice (Kanai et al., 2000) and brain-specific *Kif5b*-KO mice (Y. Tanaka and N. Hirokawa, unpublished data) do not show epileptic seizure. These data suggest a specific role of KIF5A in $GABA_AR$ transport, which cannot be compensated by KIF5B or KIF5C. Thus, to gain an insight into the KIF5A-specific $GABA_AR$-trafficking mechanism, we carried out yeast two-hybrid screening to identify proteins that interacted with KIF5A. KIF5A has 73 amino acids that have no homology with KIF5B or KIF5C (Figure 4A). Using this region as bait, we identified a clone that encoded $GABA_AR$-associated protein (GABARAP) (Wang et al., 1999) as a binding partner for KIF5A (Figure 4B). Yeast two-hybrid experiments using deletion constructs of KIF5A, KIF5B, or KIF5C revealed that the C-terminal 73 amino acids of KIF5A were sufficient for the interaction. KIF5B/KIF5C did not bind to GABARAP (Figure 4B). Interactions were also detected between KIF5A and other GABARAP family members, namely GABARAP-L1 and GABARAP-L2 (Figure 4C). The KIF5A-GABARAP interaction was further confirmed by a direct binding assay with purified recombinant proteins (Figure 4D). Recombinant KIF5A showed an interaction with GABARAP, whereas recombinant KIF5B/KIF5C did not.

The binding between KIF5A and GABARAP in vivo was further assessed by coimmunoprecipitation experiments using brain lysates (Figure 4E). Endogenous KIF5A was coimmunoprecipitated with endogenous GABARAP and $GABA_AR$. Interestingly, HAP1 was not immunoprecipitated by an anti-GABARAP antibody (Figure 4E) but was coimmunoprecipitated with $GABA_AR$ (Figure 4F) as reported previously by Twelvetrees et al. (2010). GABARAP was not immunoprecipitated with an anti-HAP1 antibody (Figure 4G). These data suggest that the KIF5A-GABARAP complex is distinct from the KIF5-HAP1 complex (Twelvetrees et al., 2010).

To examine the relationship of KIF5A with GABARAP, we studied the subcellular localization of KIF5A and GABARAP in cortical neurons by immunocytochemistry. Cells were briefly treated with saponin before fixation to reduce background signals (Nakata and Hirokawa, 1995). Significant colocalization of KIF5A puncta with GABARAP puncta was revealed by double immunolabeling (Figures 4H–4O). These data suggest that KIF5A interacts with GABARAP in WT neurons.

Next, the localization of GABARAP in the dendrites of *Kif5a*-KO neurons was analyzed. The total signal density did not vary between WT and *Kif5a*-KO neurons (<100 μm from the cell body) (genotype, density [arbitrary unit, a.u.]; WT, 52.4 ± 4.9; KO, 45.0 ± 5.0) (n = 30 neurons from three mice, mean ± SEM)

(B) mIPSC amplitude.
(C) mIPSC frequency.
(D) mIPSC 10%–90% rise time.
(E) mIPSC decay time.
(F) Cumulative probability curves for mIPSC amplitudes.
(G) Cumulative probability curves for mIPSC frequency.
(H) eIPSCs from pyramidal cells in the hippocampal CA1 region. Upward traces show eIPSCs recorded at a holding potential of 0mV, and downward traces show responses of AMPA receptors.
(I) Ratio of eIPSC amplitude to AMPA receptor-mediated eEPSCs. For all experiments, 15 slices from five mice per genotype were used (*$p < 0.01$, Student's t test). Error bars represent mean ± SEM.
(J and K) Epileptiform activity in response to stimulation in standard ACSF. (J) Population spikes in the CA1 stratum pyramidale in response to Schaffer collateral stimulation. (K) Number of population spikes.
(L) Amplitude for the first population spike.
(M and N) Epileptiform activity elicited by omission of $Mg^{2+}$ from the ACSF. (M) Population spikes in the CA1 stratum pyramidale in response to Schaffer collateral stimulation. (N) Number of population spikes.
(O) Amplitude for the first, second, third, and fourth population spike. Twelve slices from four mice per genotype were evaluated (*$p < 0.01$, Student's t test). Error bars represent mean ± SEM.

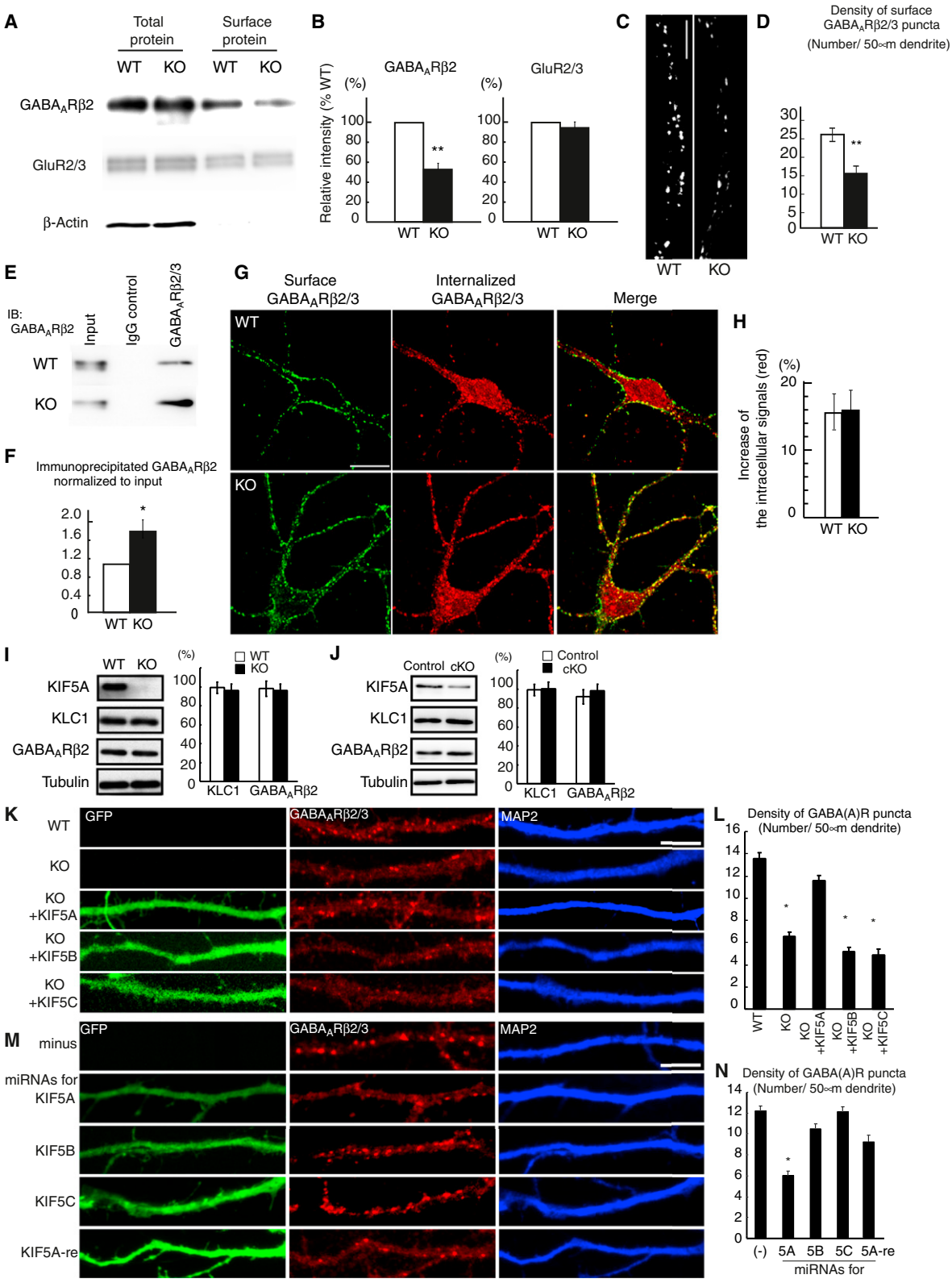


**Figure 3. Reduced Cell Surface Expression of GABA$_A$Rs in *Kif5a*-KO Hippocampal Neurons**

(A) Cell surface expression of proteins in WT and *Kif5a*-KO hippocampal neurons. The amount of cell surface GABA$_A$Rβ2 was significantly reduced in KO neurons, whereas that of GluR2/3 was unchanged.

(Figures 5A and 5B). However, the distribution of GABARAP was significantly different between genotypes. In WT cortical neurons, a punctate staining pattern of GABARAP was observed throughout dendritic processes, as reported previously by Wang et al. (1999). In *Kif5a*-KO neurons, punctate staining tended to localize in the proximal region of dendrites, compared with that in the WT; distance from the cell body, 50–75 μm (12.8 ± 0.6; 6.5 ± 0.5); 75–100 μm (11.6 ± 0.8; 5.9 ± 0.4) ($p < 0.05$; Mann-Whitney U test) (Figures 5A and 5B). These data indicate that KIF5A is involved in determining the localization of GABARAP in dendrites.

Because GABARAP was first identified as a direct binding partner for the GABA$_A$Rγ2 subunit (Wang et al., 1999), we observed γ2 subunit distribution in hippocampal neurons by immunocytochemistry. In WT neurons, many of the γ2 subunit signals colocalized with those of glutamic acid decarboxylase (GAD), an inhibitory synapse marker (Figure 5C, left panel). The number and size of synaptic γ2 subunit-positive puncta were reduced in *Kif5a*-KO neurons compared with that in WT neurons (Figure 5C, arrows in right panel). The localization of excitatory synapse markers, *N*-Methyl-D-aspartic acid (NMDA) receptor subunit (NR2B) and PSD95, showed no significant differences between genotypes (Figures 5E and 5F). Localization of inhibitory synapse marker gephyrin (Maas et al., 2009) and presynaptic marker synaptophysin was also indistinguishable between genotypes (Figures 5G and 5H). These data suggest that, although KIF5A acts at inhibitory synapses, it is not involved in gephyrin trafficking.

To investigate the possible alteration of GABA$_A$R transport in *Kif5a*-KO neurons, we carried out live imaging of neurons transfected with GABA$_A$Rγ2 subunits tagged with green fluorescent protein (GFP) (Twelvetrees et al., 2010) (Figure 6; Movie S4). Time-lapse recordings revealed that many fluorescent particles (>50%) were moving in WT neurons (Figure 6C). The velocity of anterogradely transported particles was 0.33 ± 0.02 μm/s (Figure 6D). Conversely, in *Kif5a*-KO neurons, fewer particles were moving (~25%; $p < 0.001$, chi-square test), and the velocity of anterogradely transported particles was decreased (0.11 ± 0.01 μm/s, $p < 0.05$; one-way ANOVA and post hoc test) (Figures 6B–6D). These results suggest that KIF5A is involved in active transport of GABA$_A$Rs in neurons. We observed transport of the NR2B subunit tagged with enhanced (E)GFP. The movement of NR2B-EGFP was unchanged in *Kif5a*-KO neurons compared with that in WT neurons (Figure S5; Movie S5). We examined localization of dynein, a major minus-end-directed molecular motor on microtubules. Major changes in dynein localization were not observed between WT and *Kif5a*-KO neurons (Figures S4C and S4D).

Next, to examine the role of GABARAP in GABA$_A$R transport, we performed knockdown of GABARAP in WT neurons with an miRNA vector (Figure 6; Movie S4). Specificity and efficiency of the knockdown effect of the vector are summarized in Figure S2C. Knockdown of GABARAP had a significant effect on the number of moving particles (Figure 6C), and the velocities of anterogradely transported GABA$_A$R particles were greatly reduced (Figure 6D). These results suggest a role of GABARAP in active transport of GABA$_A$Rs in neurons.

To further investigate a link between KIF5A and GABARAP, we examined the effect of GABARAP knockdown on complex formation of KIF5A with GABA$_A$Rs by immunoprecipitation. The amount of KIF5A immunoprecipitated by an anti-GABA$_A$Rβ2/3 antibody was significantly reduced when GABARAP was knocked down in neurons (Figures 7A and 7B).

To examine whether the KIF5A-GABARAP interaction was involved in GABA$_A$R trafficking, we introduced a KIF5A dominant-negative construct, KIF5A955-1027-EGFP, which corresponded to Δ2 (GABARAP-BD in Figure 4B)-EGFP, into neurons. This construct contained the GABARAP-binding site but lacked the motor domain and HAP1-BD. After transfection of the construct, surface biotinylation experiments were carried out, and a significant reduction of cell surface GABA$_A$Rβ2/3 expression was observed in neurons transfected with GABARAP-BD-EGFP (Figures 7C and 7D). These data suggest that the KIF5A-GABARAP interaction is important for GABA$_A$R trafficking to the neuronal surface.

(B) Statistics of the cell surface expression in (A) (normalized to total protein for each receptor, n = 4 independent experiments for each genotype, $^{**}p < 0.01$; Welch's t test). An absence of intracellular protein (actin) signals verified the purity of the cell surface protein fraction.
(C) Immunofluorescence staining of hippocampal neurons showed a decrease of cell surface GABA$_A$Rβ2/3 expression. Scale bar represents 10 μm.
(D) Statistics of immunofluorescence staining in (C) (n = 8 neurons from three mice for each genotype, $^{**}p < 0.01$; Student's t test).
(E) The intracellular amount of GABA$_A$Rs was increased in *Kif5a*-KO neurons, suggesting that a higher amount of GABA$_A$R protein remained in the intracellular pools in *Kif5a*-KO neurons.
(F) Statistics in (E) (n = 3 independent experiments, $^{*}p < 0.05$; Welch's t test).
(G and H) Endocytosis assay of cell surface GABA$_A$Rs. Cell surface GABA$_A$Rβ2/3 was labeled with an Alexa Fluor 488-conjugated secondary antibody, whereas endocytosed GABA$_A$R was labeled with an Alexa Fluor 568-conjugated secondary antibody. Kinetics of GABA$_A$R endocytosis was indistinguishable between WT and *Kif5a*-KO hippocampal neurons (n = 6 neurons from three mice for each genotype). Scale bar represents 10 μm. Error bars represent mean ± SEM.
(I and J) Western blot analysis of proteins. (I) WT and *Kif5a*-KO mouse brain lysates (embryonic day 18). (J) Control and *Kif5a*-conditional KO mouse brain lysates (postnatal day 16). Error bars, mean ± SEM (n = 3).
(K and L) Rescue of reduced cell surface GABA$_A$R expression in *Kif5a*-KO neurons. (K) Hippocampal neurons were transfected with EGFP-tagged full-length expression vectors for KIF5A, KIF5B, or KIF5C. At 48 hr posttransfection, neurons were fixed and stained with antibodies against GABA$_A$Rβ2/3 and MAP2. Cell surface GABA$_A$R expression in the dendrites of *Kif5a*-KO neurons was reduced. This reduction was rescued by transfection of the KIF5A expression vector but was not by those for KIF5B or KIF5C. (L) Statistics of immunofluorescent signals in (K) (compared with that of the WT, n = 15 neurons for each construct, $^{*}p < 0.05$; Student's t test).
(M and N) Knockdown of KIF5s. (M) Hippocampal neurons were cotransfected with miRNAs against each KIF5 and an EGFP expression vector that served as an expression marker. At 72 hr posttransfection, neurons were fixed and stained with antibodies against GABA$_A$Rβ2/3 and MAP2. KIF5A-re, coexpression of a KIF5A miRNA with an miRNA-resistant KIF5A cDNA, restored GABA$_A$Rβ2/3 localization in dendrites. (N) Statistics of immunofluorescent signals in (M) (compared with that of nontransfected cells [minus], n = 15 neurons for each miRNA construct, $^{*}p < 0.05$; Student's t test). Scale bars represent 10 μm.
Related to Figures S2–S4.

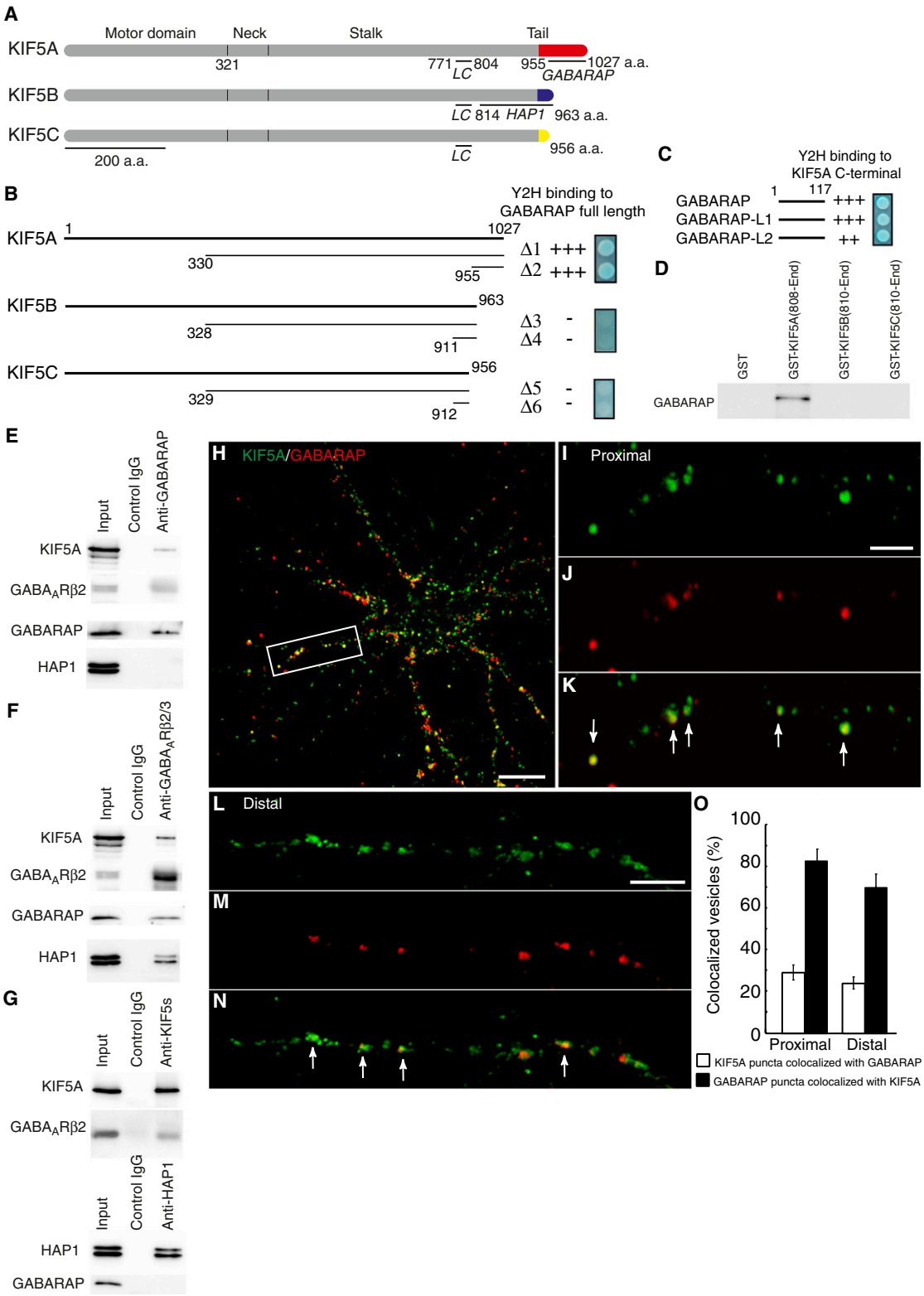


**Figure 4. KIF5A Specifically Binds to GABARAP in Neurons**

(A) Schematic diagram of KIF5s. Three KIF5s show a very high degree of homology in their entire length, but each KIF5 has a short sequence with very few similarities at their C-terminal cargo-BD (red for KIF5A, blue for KIF5B, and yellow for KIF5C). Bars represent regions for each binding protein. *LC*, kinesin light chain.

Next, to examine the role of the KIF5A-GABARAP pathway and the previously reported KIF5-HAP1 pathway (Twelvetrees et al., 2010) in surface expression of GABA$_A$Rs, we tested the effect of knockdown of GABARAP or HAP1 on cell surface expression of GABA$_A$Rβ2/3 in hippocampal neurons. Knockdown levels were similar between the two miRNAs (Figures S2C and S2D). Both miRNA vectors reduced total, synaptic (overlapped with synaptophysin signals), and extrasynaptic (not overlapped with synaptophysin signals) cell surface GABA$_A$Rβ2/3 levels (Figures 7E and 7F). In HAP1-knockdown neurons, the reduction tended to be more evident in the levels of extrasynaptic GABA$_A$Rβ2/3 (Figures 7E and 7F). These results suggest that both KIF5A/GABARAP and KIF5/HAP1 complexes are important for surface and synaptic localization of GABA$_A$Rs.

### Involvement of KIF5A in Post-Golgi Trafficking of GABA$_A$Rs in Neurons

To further investigate the dynamic process of GABA$_A$R transport, we observed the endoplasmic reticulum (ER)-to-Golgi and post-Golgi dynamics of GABA$_A$Rγ2-GFP in neurons. GABA$_A$Rγ2-GFP was diffusely distributed in the somatodendritic area when expressed in the presence of brefeldin A (BFA) (Figure 8A). At 1 hr after BFA washout, GABA$_A$Rγ2-GFP accumulated in the Golgi apparatus in neurons from mice of each genotype (Figures 8A and 8C), suggesting that ER-to-Golgi transport of GABA$_A$Rs was unaffected. Importantly, less GABA$_A$Rγ2-GFP clusters tended to be distributed in the dendrites of neurons from KIF5A-KO mice at 2, 2.5, and 3 hr after the washout, which was possibly because of the impairment of post-Golgi transport of GABA$_A$Rγ2-GFP (Figures 8A and 8D).

Next, we compared surface expression of GABA$_A$R-GFP in dendrites after BFA treatment and washout between *Kif5a*-KO and WT mouse neurons. We visualized surface-expressed GABA$_A$R-GFP by immunocytochemistry. After washout of BFA, cells were fixed and incubated with an anti-GFP antibody without permeabilization. Because the GFP tag of the GABA$_A$R-GFP construct is located at the outer surface after membrane insertion (Kittler et al., 2000), we could detect the surface receptor using this procedure. As a result, we observed a significant delay in surface expression of GABA$_A$R-GFP in *Kif5a*-KO neurons (Figures 8B and 8E).

We tried to further characterize the alteration of GABA$_A$R transport in *Kif5a*-KO mouse neurons by comparing the glycosylation state of GABA$_A$Rs between genotypes. GABA$_A$Rs are known to be heavily glycosylated in neurons, and some mutations of GABA$_A$R subunits have been reported to be involved in the receptor glycosylation state that can affect the intracellular fate of GABA$_A$Rs (Lo et al., 2010; Tanaka et al., 2008). We performed a glycosylation assay of conditional *Kif5a*-KO and control mouse brain lysates using two enzymes; endoglycosidase H (EndoH), which only digests immature high-mannose sugar, and peptide N-glycosidase F (PNGaseF), which removes all N-linked carbohydrates (Tomita et al., 2003). As a result, digested band patterns of GABA$_A$Rβ2/3 and GluR2/3 were similar between genotypes (Figure 8F), indicating that the glycosylation state of these receptors was not significantly different between genotypes and that the GABA$_A$Rs were fully glycosylated in conditional *Kif5a*-KO cells. Considering that de novo synthesized proteins are glycosylated in the ER and Golgi apparatus, this result suggests that KIF5A is involved in the post-Golgi trafficking of GABA$_A$Rs, but not in pre-Golgi and intra-Golgi pathways of GABA$_A$R transport.

## DISCUSSION

### KIF5A and Inhibitory Neural Transmission

We found an abnormal EEG in the hippocampus of KIF5A-deficient mice. The waveforms represented paroxysms, and spikes and waves were considered to be a typical epileptic discharge (Figures 1F–1H). Such abnormal waveforms are caused by impairment of GABA$_A$R-mediated neurotransmission (Jacob et al., 2008). Consistently, we found an impairment of mIPSCs and eIPSCs together with increased neuronal excitability (Figure 2) and reduced cell surface expression of GABA$_A$Rs in KIF5A-deficient mice (Figure 3). These results emphasize the role of KIF5A protein in GABA$_A$R trafficking. On the other hand, a static pattern with low amplitudes was observed in the baseline EEG of KIF5A-deficient mice (Figures 1B–1E). This observation is paradoxical because, in the simplest interpretation, impairment of GABAergic neurotransmission is considered to increase excitatory signals and cause higher amplitudes of the EEG (Elsen et al., 2006). In the mammalian central nervous system, inhibitory neurotransmission is mediated mainly via GABA$_A$Rs that are responsible for maintaining EEG power by synchronizing neural network activity. Indeed, a blockade of GABA$_A$Rs results in the loss of synchronization of EEG power (Porjesz et al., 2002; Tobler et al., 2001). We speculate that the baseline EEG with low amplitudes in *Kif5a*-KO mice (Figures 1J and 1K) was a result of reduced synchronism due to a defect in the inhibitory neural network. In conclusion, our results demonstrate that KIF5A is an important molecular component in maintaining neuronal network activity via the transport of GABA$_A$Rs.

### Specific Role of KIF5A in GABA$_A$R Transport

Our data indicate that GABARAP is a link between KIF5A and GABA$_A$R. This link was specific for KIF5A, whereas KIF5B and KIF5C did not bind to GABARAP (Figure 4). Among proteins

(B and C) Yeast two-hybrid assay. (B) KIF5A binds to GABARAP, whereas KIF5B and KIF5C do not. (C) The KIF5A C-terminal region, which has no homology with KIF5B or KIF5C, binds to GABARAP, GABARAP-L1, and GABARAP-L2.

(D) Direct binding assay with purified recombinant KIF5s and GABARAPs.

(E–G) Immunoprecipitation of a mouse brain lysate. KIF5A coimmunoprecipitates with GABARAP (E) and GABA$_A$R (F). HAP1 coimmunoprecipitates with GABA$_A$R (F), but not with GABARAP (E and G). GABA$_A$R is coimmunoprecipitated with an antibody against all KIF5s (SUK4), which mainly binds to KIF5A (Kanai et al., 2000) (G).

(H–O) Immunofluorescence staining of KIF5A and GABARAP shows colocalization of both molecules in cortical neurons. KIF5A (green) and GABARAP (red) colocalize in neuronal processes. Images shown in (I)–(K) are magnifications of the boxed region in (H). Scale bars represent 20 μm (H), 5 μm (I), and 10 μm (L). Arrows in (K) and (N) indicate colocalized puncta of KIF5A and GABARAP. (O) Statistics of the colocalization. Error bars represent mean ± SEM (n = 12).

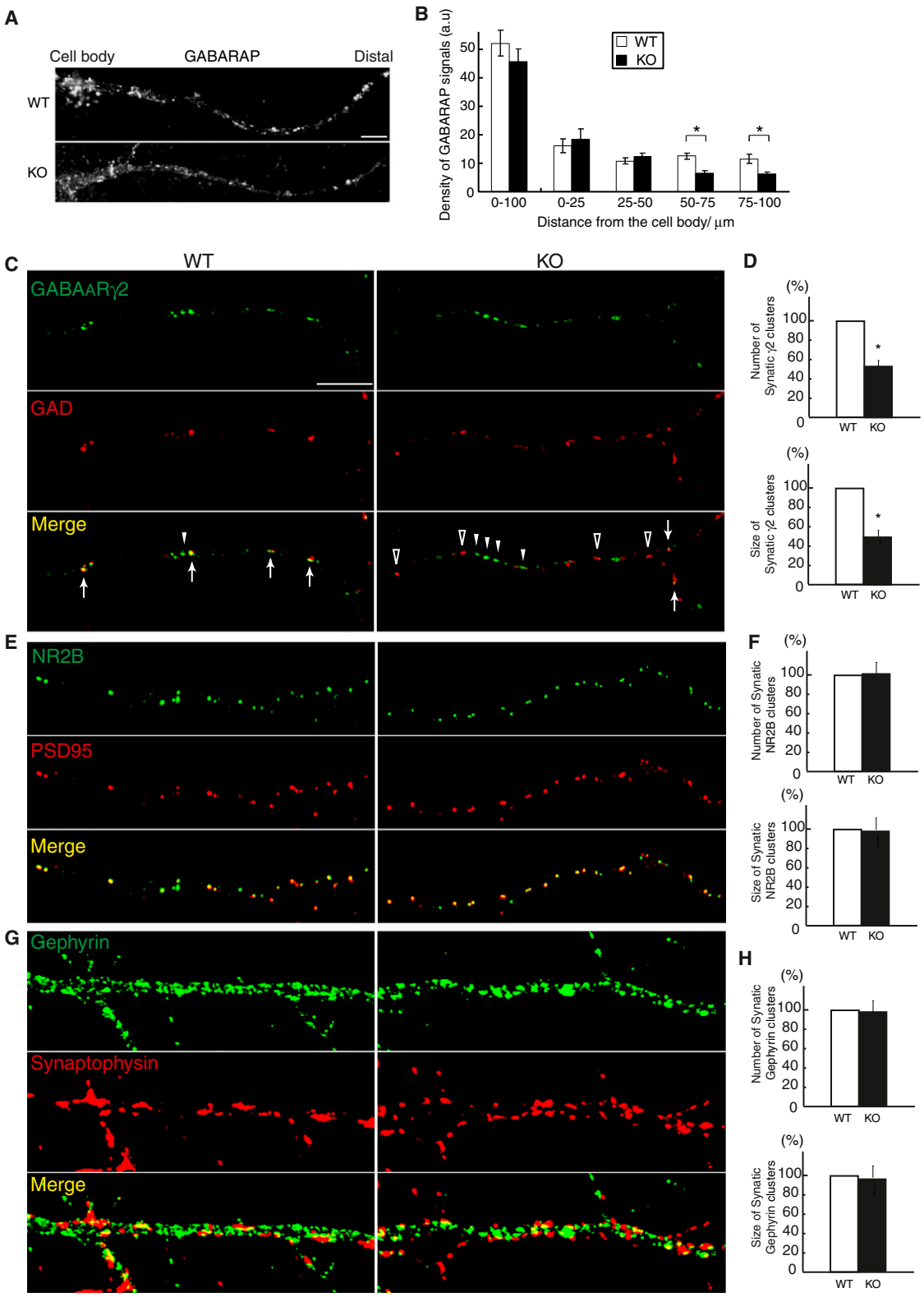


**Figure 5. Immunofluorescence Analysis of KIF5A-KO Neurons**

(A) Immunofluorescence staining of GABARAP in KIF5A WT and *Kif5a*-KO cortical neurons. Scale bar represents 10 μm.

(B) Statistics of the distribution of GABARAP signals (three experiments, n = 30 neurons, *p < 0.05; Mann-Whitney U test). Error bars represent mean ± SEM.

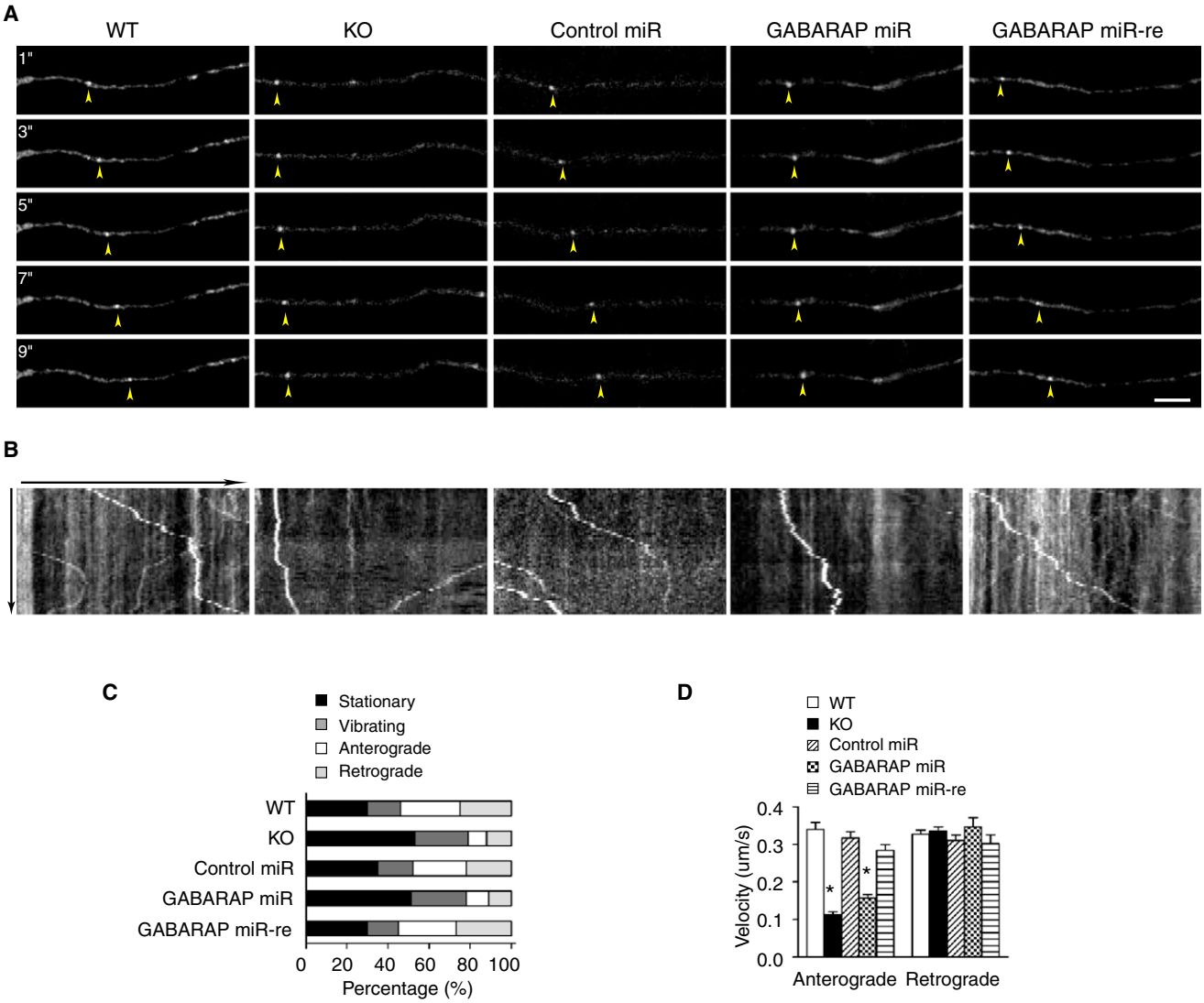


**Figure 6. Analysis of GFP-Tagged GABA$_A$R Dynamics in Neurons**

(A) Time-lapse images of GFP-tagged GABA$_A$R vesicles in dendrites. Yellow arrows indicate anterogradely moving vesicles. Scale bar represents 5 μm.

(B) Kymograph showing the motility of GABA$_A$R vesicles. x axis, 30 μm; y axis, 100 s.

(C) Classification of motility ($p < 0.001$; chi-square test).

(D) Average velocities for anterograde and retrograde movement of vesicles. Error bars represent mean ± SEM (n = 38 neurons from three mice/genotype, *$p < 0.05$; one-way ANOVA and post hoc test).

Related to Figures S2, S4, and S5, and Movies S4 and S5.

reported to bind directly to KIF5s, Myo5A is specific for KIF5B (Huang et al., 1999). However, there has been no report of a specific binding partner for KIF5A or KIF5C. GABARAP is an example of a protein that specifically interacts with KIF5A. GABARAP was originally identified as a direct binding protein of the GABA$_A$R$\gamma$2 subunit (Wang et al., 1999) and is involved in GABA$_A$R trafficking in neurons (Kittler et al., 2001; Leil et al., 2004; Marsden et al., 2007). However, the mechanism by which GABARAP controls GABA$_A$R trafficking in association with the microtubule cytoskeleton has been unclear (Wang and

(C) GABA$_A$R$\gamma$2 and GAD staining in hippocampal neurons. Arrows indicate colocalized puncta. Solid arrowheads denote extrasynaptic GABA$_A$R$\gamma$2. Open arrowheads show GAD signals without GABA$_A$R$\gamma$2.

(D) Statistics in (C).

(E) NR2B and PSD95 staining in hippocampal neurons.

(F) Statistics in (E).

(G) Gephyrin and synaptophysin staining in hippocampal neurons.

(H) Statistics in (G). (n = 10, *$p < 0.05$; Student's t test).

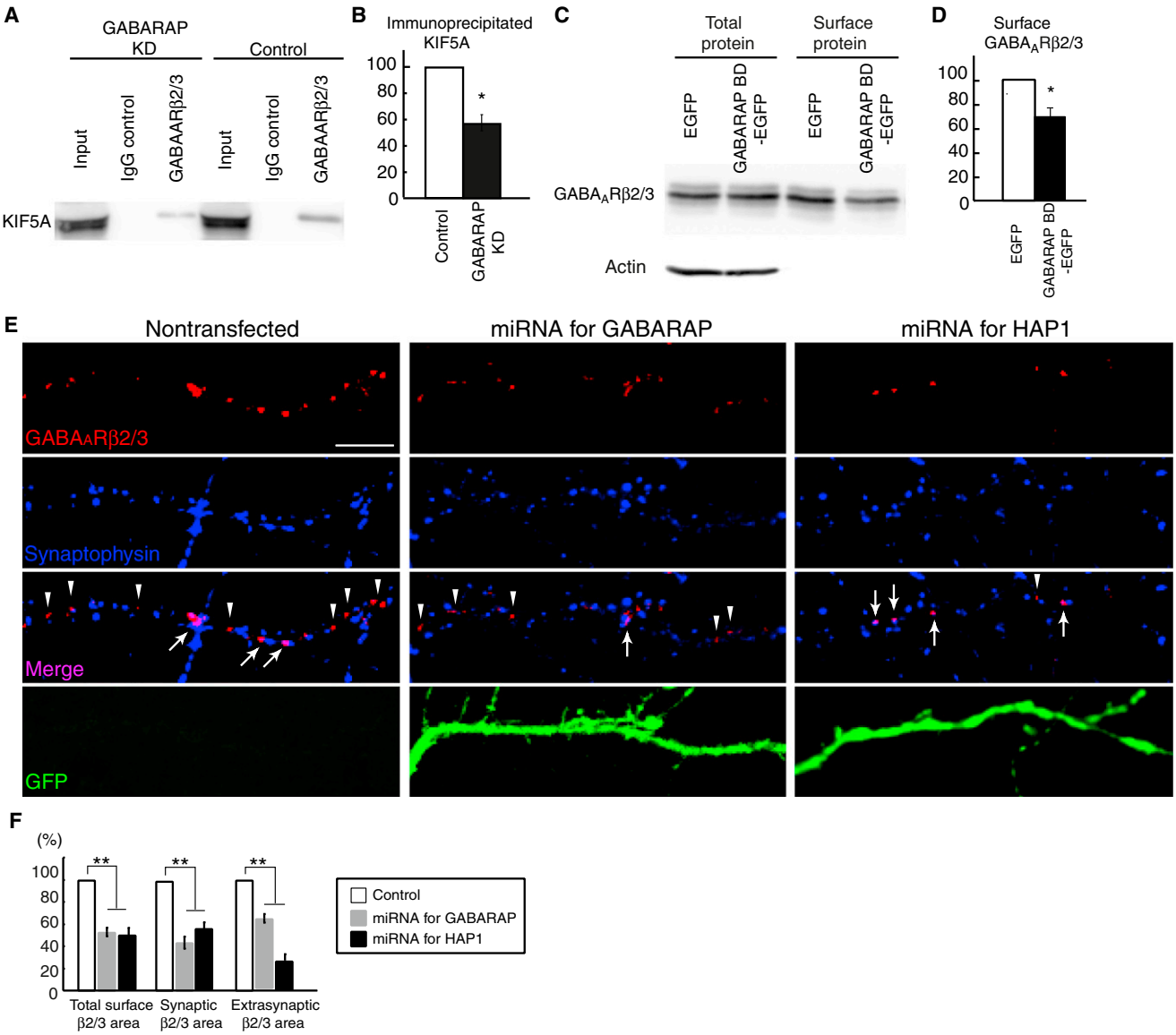


**Figure 7. KIF5A-GABARAP Pathway Is Involved in GABA$_A$R Trafficking to the Neuronal Surface, which Is Distinct from the KIF5-HAP1 Pathway**

(A and B) Reduced coimmunoprecipitation of GABA$_A$Rβ2/3 and KIF5A in GABARAP knocked down (KD) cortical neurons. Control, only EGFP was transfected. (A) Western blots. (B) Statistics of the amount of immunoprecipitated KIF5A (normalized to the amount of input) in (A) (n = 3 independent experiments, *p < 0.05; Student's t test).

(C and D) Overexpression of the KIF5A C-terminal fragment (Δ2 in Figure 4B, which was bound to GABARAP) resulted in reduced cell surface GABA$_A$R expression in WT cortical neurons. (C) Western blot analysis of cell surface proteins. (D) Statistics of cell surface expression in (C) (normalized to total amount, n = 3 independent experiments, *p < 0.05; Student's t test). Error bars represent mean ± SEM.

(E and F) Knockdown of GABARAP or HAP1 in neurons. (E) Hippocampal neurons were cotransfected with miRNAs against GABARAP or HAP1, and an EGFP expression vector that served as an expression marker. At 72 hr posttransfection, neurons were fixed and stained with antibodies against GABA$_A$Rβ2/3 and synaptophysin. Scale bar represents 10 μm. (F) Statistics of immunofluorescent signals in (E) (compared with that of nontransfected cells, n = 15 neurons from three independent cultures for each miRNA construct, **p < 0.01; Student's t test).

Related to Figure S2.

Olsen, 2000). In this study, we clarified that microtubule-dependent mechanisms via KIF5A are important for GABARAP to function in GABA$_A$R transport in neurons. KIF5A binds to and transports GABARAP, and the interaction regulates the trafficking of GABA$_A$Rs in neurons (Figures 4, 5, 6, 7, and 8). KIF5A appropriately arranges GABARAP throughout dendrites, and GABA$_A$R complexes may be transported to the plasma membrane via anchorage to distribute GABARAP. Alternatively,

KIF5A may transport GABARAP/$GABA_AR$ as a complex to an appropriate intracellular compartment, which facilitates $GABA_AR$ trafficking to the plasma membrane. We propose that these two possibilities are compatible with each other.

It should be noted that simple diffusion would be involved in the intracellular translocation of GABARAP considering its small molecular weight (less than 20 kDa). Therefore, it is possible that a proportion of GABARAP can move into dendrites even when KIF5A-mediated active transport is disrupted. However, it would be insufficient to support the long-distance delivery of $GABA_AR$s, leading to the significant $GABA_AR$-related phenotypes in *Kif5a*-KO mice. It is also possible that the phenotypes in *Kif5a*-KO neurons would be partly because the GABARAP molecules are not properly arranged or anchored for efficient trafficking of $GABA_AR$s to the neuronal surface.

## Multiple Roles of KIF5s in $GABA_AR$ Trafficking

The KIF5-HAP1 complex has been reported to be involved in the transport of $GABA_AR$s (Twelvetrees et al., 2010). The KIF5A-GABARAP complex does not contain HAP1 (Figures 4E and 4G). HAP1 resides in early endosomes containing $GABA_AR$s (Twelvetrees et al., 2010). In contrast, GABARAP is localized to the Golgi apparatus and somatodendritic membrane compartments, except at synapses (Luscher et al., 2011). Knockdown of GABARAP or HAP1 greatly reduced the surface $GABA_AR$ clusters both in synaptic and extrasynaptic regions (Figures 7E and 7F). Accordingly, we showed that the KIF5A-GABARAP pathway participated in post-Golgi transport to distal dendrites (Figures 8A and 8B), whereas the KIF5-HAP1 complex facilitates trafficking of $GABA_AR$s from early endosomes to the plasma membrane (Twelvetrees et al., 2010). Thus, the two mechanisms may cooperatively constitute an orchestrated mechanism of $GABA_AR$ transport in neurons.

On the other hand, microtubule tracks as well as actin filaments would be important for synaptic delivery of $GABA_AR$s because actin cytoskeletons are major structural components of the juxtamembrane region. Recently, multidomain protein Muskelin has been identified as an essential factor for cell surface $GABA_AR$ expression and has been shown to interconnect with actin- and microtubule-based transport of $GABA_AR$s (Heisler et al., 2011). Thus, GABARAP, HAP1, and Muskelin should work as trafficking factors together with molecular motors for transport of $GABA_AR$s to the neuronal surface and synapses. Interestingly, GABARAP-KO mice do not show phenotypes related to $GABA_AR$ dysfunction (O'Sullivan et al., 2005). This observation is probably due to functional compensation by its homolog GABARAP-L1, because both proteins are capable of binding to the $GABA_AR$ γ2 subunit (Mansuy et al., 2004) and mRNA expression levels of GABARAP-L1 are higher than those of GABARAP in some areas of rat brain (Mansuy-Schlick et al., 2006). Our results show that KIF5A interacts with both proteins (Figure 4C), and the loss of KIF5A protein results in severe $GABA_AR$-related phenotypes.

## KIF5A and Human Hereditary Spastic Paraplegia

Spastic paraplegia (SPG) is a diverse group of inherited disorders characterized by progressive lower-extremity spasticity and weakness. Several mutations in the *KIF5A* gene have been identified in the genomic DNA of affected families (Fichera et al., 2004; Reid et al., 2002). SPGs with *KIF5A* mutations are classified as *SPG10* that is characterized by sensory-motor neuropathy, presumably because of abnormal accumulation of NFs. Importantly, patients with *SPG10* do not show epileptic symptoms (Fichera et al., 2004; Musumeci et al., 2011). In striking contrast, the central feature of the conditional *Kif5a*-KO mouse is severe epilepsy, and neither axonopathy nor NF accumulation is observed in their nervous system. This discrepancy can be partly explained by the death of conditional *Kif5a*-KO mice at an early stage (~3 weeks old), in which no significant accumulation of NF proteins is observed (Figure S3). In another *Kif5a*-KO mouse line, one-fourth survived until 5.5 months and showed abnormal NF transport (Xia et al., 2003). Thus, our *Kif5a* mutant mouse may be useful to study presymptomatic states of *SPG10*.

In summary, we characterized epileptic seizures observed in conditional *Kif5a*-KO mice by EEG recording and found that $GABA_AR$ trafficking to the neuronal surface is impaired in the KIF5A-deficient neurons, which was confirmed by electrophysiology. We identified GABARAP as a direct and specific binding partner of KIF5A. The KIF5A-GABARAP interaction was shown to be involved in abnormal trafficking of $GABA_AR$s, which may provide a molecular mechanism that explains the phenotypes observed in *Kif5a*-KO mice and an insight into the role of KIF5A in inhibitory synaptic transmission (Figures 8G and 8H).

## EXPERIMENTAL PROCEDURES

Detailed procedures are provided in the Supplemental Experimental Procedures.

### Gene Targeting of the Kif5a Gene

A 3*loxP*-type targeting vector was constructed using a genomic clone obtained from a λEMBL3 genomic library and genomic fragments amplified from the 129/Sv-derived embryonic stem cell (ESC) line CMT1-1 (Chemicon/Millipore, Billerica, MA, USA) with an LA-PCR kit (Takara, Japan) as schematically shown in Figure S1A. Electroporation was carried out as described elsewhere (Joyner, 1993; Nakajima et al., 2002). By crossing 3*loxP*/+ male mice with female *CAG-Cre*$^{tg/•}$ transgenic mice (Sakai and Miyazaki, 1997), the selection cassette and exons, flanked by *loxP* sequences, were removed to obtain 1*loxP*/+ mice (*Kif5a*$^{+/-}$ allele). *Kif5a*-KO mice (*Kif5a*$^{-/-}$ allele) were generated by intercrossing these mice. For conditional gene targeting, 3*loxP*/+ ESCs were electroporated with a pCre-Pac plasmid (Taniguchi et al., 1998) to remove the selection cassette flanked by *loxP* sequences. 2*loxP*/+ ESCs were injected into blastocysts to obtain 2*loxP*/+ mice (*Kif5a*$^{fl/+}$ allele) that were intercrossed to produce *Kif5a*$^{fl/fl}$ mice. Synapsin promoter-driven *Cre* transgenic mice (*Syn-Cre*$^{tg/•}$) (Zhu et al., 2001) were used to conditionally delete exons flanked by *loxP*. The detailed procedure is provided in the Supplemental Experimental Procedures.

### EEG Recording

Control and conditional KO mice (postnatal days 14–20) were anesthetized with ketamine/xylazine and surgically implanted with a set of electrodes; two 0.1-mm-diameter silver wires were bonded; one was a 1.2-mm-long reference electrode, and the other was a 2.0-mm-long working electrode with a hard epoxy resin coat except for the 0.2-mm-long exposed tip to electrically insulate from the reference electrode. The detailed procedure is provided in the Supplemental Experimental Procedures.

### Electrophysiology of Brain Slice Cultures

Hippocampal slices were prepared as described previously (Yin et al., 2012). Mice at postnatal days 15–20 were anesthetized, decapitated, and their brains were rapidly transferred to cold oxygenated ACSF consisting of 119 mM NaCl,

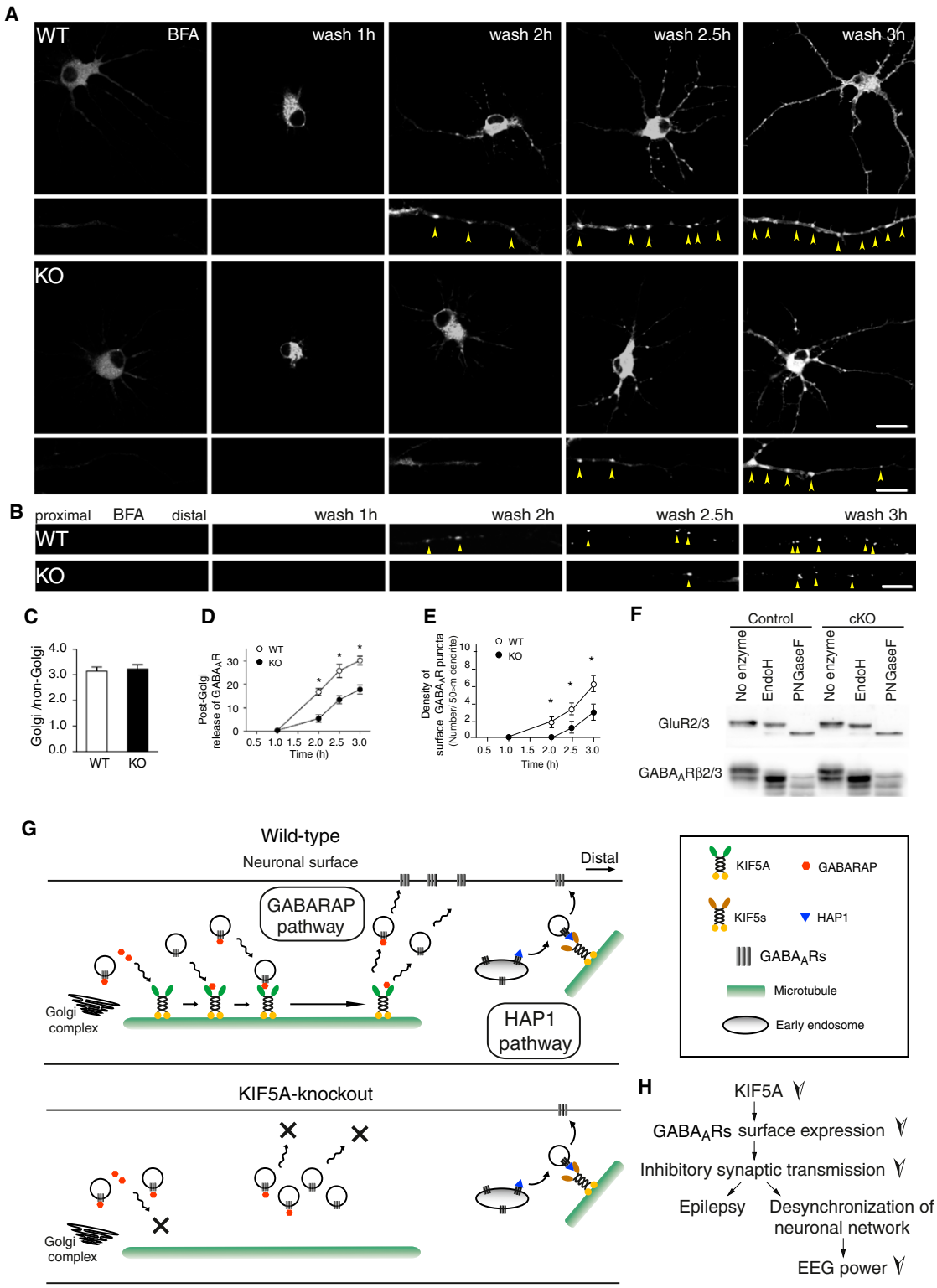


**Figure 8. KIF5A Is Involved in Post-Golgi Trafficking of GABA$_A$R**

(A–E) ER-to-Golgi and post-Golgi transport of GFP-tagged GABA$_A$R in neurons. (A) Dynamics of GFP-tagged GABA$_A$R after BFA washout (wash). Hippocampal cultures were cotransfected with α1, β3, and GFP-γ2 constructs. Images were acquired at the indicated time points after BFA washout. Scale bar represents 20 μm for whole-cell images and 10 μm for neurite images. (B) Immunocytochemistry of surface-expressed GFP-tagged GABA$_A$R. Scale bar, 10 μm. (C) The fluorescent intensities of the Golgi and non-Golgi were expressed as ratios at 1 hr after BFA washout (mean ± SEM., $p > 0.05$; Student's t test). (D) Percentage of

2.6 mM KCl, 1.3 mM $MgSO_4$, 1 mM $NaH_2PO_4$, 26 mM $NaHCO_3$, 2.5 mM $CaCl_2$, and 11 mM D-glucose. Slices (400 μm) were cut transversely with a Leica VT1200S and kept at 34°C for at least 1 hr before recording.

Field potentials were recorded extracellularly in the CA1 area of slices. For each slice, a bipolar electrode was placed in the stratum radiatum, and the Schaffer collateral pathway was stimulated at a frequency of 0.1 Hz using constant current pulses of 0.1 ms. Stimulus-evoked population spikes were recorded using a borosilicate glass microelectrode (filled with 1 M NaCl) positioned in the stratum pyramidale. To examine hyperexcitability, epileptiform activity was recorded in $Mg^{2+}$-free ACSF.

Whole-cell patch-clamp recordings in CA1 pyramidal neurons were performed at room temperature with an Axopatch 1D amplifier (Axon Instruments, Union City, CA, USA). Patch pipettes (3–5 MΩ) were filled with 122.5 mM Cs gluconate, 17.5 mM CsCl, 10 mM HEPES, 0.2 mM EGTA, 8 mM NaCl, 2 mM Mg-ATP, and 0.3 $Na_3$-GTP (pH 7.2, 290–300 mM mOsm). All $GABA_AR$-mediated currents were recorded in the presence of 50 μM D-2-amino-5-phosphonovaleric acid (Tocris, Bristol, UK) and 10 μM 2,3-dioxo-6-nitro-1,2,3,4-tetrahydrobenzo[f]quinoxaline-7-sulfonamide (Tocris, Bristol, UK). For eIPSC recording, a bipolar-stimulating electrode was used to stimulate afferent fibers. IPSCs evoked by current pulses (0.1 ms duration) at 0.05 Hz were recorded at a holding potential of 0mV. mIPSCs were collected in the presence of 0.5 μM tetrodotoxin (Sigma-Aldrich, St. Louis, MO, USA) to block action potentials. All membrane potential values were corrected for liquid junction potentials of −11mV. Access resistance was continuously monitored throughout the experiment. Recordings were included for analysis when the series resistance was less than 20 MΩ and rejected if the series resistance changed by more than 20%. Data were filtered at 2 kHz, digitized at 10 kHz, and analyzed using the Mini Analysis Program (version 6.0; Synaptosoft, Decatur, GA, USA).

### Immunofluorescence Analysis

Hippocampal and cortical neurons from embryonic day 16.5 mouse embryos were prepared and cultured as described elsewhere by Brewer (1995) and Kaech and Banker (2006). For cell surface $GABA_AR$ staining, cells were fixed with 4% paraformaldehyde without permeabilization, blocked with 5% BSA in PBS, and incubated with a primary antibody against $GABA_AR\beta2/3$ subunits (62-3G1), which bound to the extracellular domain of the subunits, at 4°C overnight. For colocalization analysis of KIF5A and GABARAP, cortical neurons were permeabilized with 0.02% saponin in HEPES-buffered Hank's solution for 5 min at room temperature, followed by fixation with 4% paraformaldehyde and permeabilization with 0.1% Triton X-100, and then stained with an anti-KIF5A rabbit polyclonal antibody and anti-GABARAP goat polyclonal antibody (C-19). For staining of GABARAP in cortical neurons, an anti-GABARAP rabbit polyclonal antibody (FL-117) was used. Immunohistochemistry was carried out as described elsewhere by Takayama and Inoue (2003) and Xia et al. (2003). Imaging was carried out under a Zeiss LSM510 confocal laser-scanning microscope. Quantification of fluorescence images was performed using Scion Image and ImageJ software.

### Endocytosis Assay

For the endocytosis assay, internalization of $GABA_AR$ was monitored as described elsewhere by Goodkin et al. (2005) and Heisler et al. (2011). Cultures of hippocampal neurons (14–18 days in vitro) were incubated at 4°C for 1 hr in the presence of an anti-$GABA_AR\beta2/3$ antibody (clone 62-3G1). After incubation, the neurons were washed with PBS and then incubated in antibody-free medium to allow antibody-bound receptors to undergo internalization at 37°C for 90 min ($GABA_AR$ internalization was maximal at this time point), followed by fixation for 15 min with 4% paraformaldehyde. After fixation, neurons were blocked with 5% BSA for 30 min, exposed to the first of two secondary antibodies (20 μg/ml Alexa Fluor 488-conjugated goat anti-mouse) for 2 hr under a nonpermeabilized condition, and then permeabilized by treatment with 0.25% Triton X-100 for 10 min, followed by incubation with the other secondary antibody (10 μg/ml Alexa Fluor 568-conjugated goat anti-mouse) for 1 hr. Observation was carried out under a Zeiss LSM510 confocal laser-scanning microscope. Red signals represented internalized surface receptor, and green signals represented receptors that remained on the cell surface.

### Molecular Biology

Full-length cDNA clones of KIF5s had been previously obtained by Kanai et al. (2000). Yeast two-hybrid assays were performed as described elsewhere by Setou et al. (2000). The detailed procedure is provided in the Supplemental Experimental Procedures.

### Live Imaging

To perform live imaging of GFP-tagged $GABA_AR$ transport, after 7 days of culture, hippocampal neurons were transfected with α1, β3, and GFP-γ2 constructs (Twelvetrees et al., 2010). At 36–48 hr posttransfection, live neurons were observed under a Zeiss LSM710 Duo confocal laser-scanning microscope. Movement of $GABA_AR$ vesicles along dendrites was monitored over time, and images were acquired every second. Determination of the velocities was performed for 30 s. The path of individual vesicles was traced, and distances were evaluated using LSM710 software. Analysis and graphical representation were performed using ImageJ software and GraphPad Prism (GraphPad Software, San Diego, CA, USA).

### Post-Golgi Release of $GABA_AR$

To monitor post-Golgi release of $GABA_AR$ vesicles, $GABA_AR$ α1, β3, and GFP-γ2 constructs were initially expressed in hippocampal cells in the presence of 10 μg/ml BFA (Wako Pure Chemical Industries, Osaka, Japan). After extensive BFA washout, cells were observed under an LSM710 confocal laser-scanning microscope. Quantification was performed as described elsewhere (Yin et al., 2012). At 1 hr after BFA washout, three regions of interest were drawn at peripheral locations, and the corresponding mean fluorescence represented an estimation of GFP-γ2 at non-Golgi locations. Golgi-associated fluorescence was determined from perinuclear regions. To ascertain the percentage of post-Golgi release of $GABA_AR$ vesicles, we divided the fluorescence intensity outside of the Golgi area by that of the total cell area. The background was subtracted using the fluorescence intensity outside of the Golgi area. Immunocytochemistry of surface GFP-tagged receptors was performed using an anti-GFP antibody under a nonpermeabilized condition.

### Glycosylation Assay

Glycosylation assays were performed as described previously by Standley et al. (1998). Briefly, mouse whole brain (postnatal day 16) was homogenized with 1 ml homogenizing buffer (50 mM Tris-HCl [pH 7.6], 5 mM EDTA, and 10% sucrose) including a Protease Inhibitor Cocktail (Roche). Homogenates were first centrifuged at 1,000 × *g* for 10 min to yield the nuclear fraction (P1), and then the supernatant (S1) was centrifuged at 10,000 × *g* for 20 min to yield the mitochondrial fraction (P2). After resuspending the P2 fraction with the same volume of homogenizing buffer, the lysates were subjected to enzyme digestion for more than 12 hr according to the manufacturer's instructions. Both EndoH and PNGaseF were purchased from New England BioLabs (Ipswich, MA, USA).

## SUPPLEMENTAL INFORMATION

Supplemental Information includes five figures, five movies, and Supplemental Experimental Procedures and can be found with this article online at http://dx.doi.org/10.1016/j.neuron.2012.10.012.

released GFP-tagged $GABA_AR$ signals from the Golgi region. (E) Statistical analysis of the signal intensity of surface-expressed GFP-tagged $GABA_AR$ signals shown in (B). Error bars represent mean ± SEM, *p < 0.05; Student's t test. For quantification, 20 neurons from three mice of each genotype were examined.
(F) Glycosylation assay.
(G) Models of $GABA_AR$ transport by KIF5A. The KIF5A-GABARAP pathway participates in post-Golgi transport, whereas the KIF5-HAP1 complex facilitates trafficking of $GABA_AR$s from early endosomes to the plasma membrane (Twelvetrees et al., 2010).
(H) Summary of predicted pathophysiology of *Kif5a*-KO mouse phenotypes.

## ACKNOWLEDGMENTS

We are grateful to Josef Kittler (University College London), Chitoshi Takayama (University of the Ryukyus), and Masato Hirata (Kyushu University) for kindly providing the GFP-tagged $GABA_AR$ constructs, antibodies against $GABA_AR$ subunits, and plasmids for GABARAP, respectively. We also thank Yosuke Tanaka, Ying Tong, and Yayoi Kikkawa for assistance in generating the knockout mouse; Yoshimitsu Kanai, Shinsuke Niwa, and Kazuhiko Mitsumori for technical assistance; and H. Sato, H. Fukuda, N. Onouchi, T. Akamatsu, T. Aizawa, and all other members of the Hirokawa laboratory for assistance. This work was supported by a Grant-in-Aid for specially promoted research to N.H. from the Ministry of Education, Culture, Sports, Science and Technology of Japan, and by the Basic Science Research Program through the National Research Foundation of Korea, funded by the Korean Ministry of Education, Science and Technology (2012-007530, to D.-H.S.).

Accepted: October 8, 2012
Published: December 5, 2012

## REFERENCES

Brewer, G.J. (1995). Serum-free B27/neurobasal medium supports differentiated growth of neurons from the striatum, substantia nigra, septum, cerebral cortex, cerebellum, and dentate gyrus. J. Neurosci. Res. *42*, 674–683.

Elsen, F.P., Liljelund, P., Werner, D.F., Olsen, R.W., Homanics, G.E., and Harrison, N.L. (2006). GABA(A)-R alpha1 subunit knockin mutation leads to abnormal EEG and anesthetic-induced seizure-like activity in mice. Brain Res. *1078*, 60–70.

Fichera, M., Lo Giudice, M., Falco, M., Sturnio, M., Amata, S., Calabrese, O., Bigoni, S., Calzolari, E., and Neri, M. (2004). Evidence of kinesin heavy chain (KIF5A) involvement in pure hereditary spastic paraplegia. Neurology *63*, 1108–1110.

Goodkin, H.P., Yeh, J.L., and Kapur, J. (2005). Status epilepticus increases the intracellular accumulation of GABAA receptors. J. Neurosci. *25*, 5511–5520.

Heisler, F.F., Loebrich, S., Pechmann, Y., Maier, N., Zivkovic, A.R., Tokito, M., Hausrat, T.J., Schweizer, M., Bähring, R., Holzbaur, E.L., et al. (2011). Muskelin regulates actin filament- and microtubule-based GABA(A) receptor transport in neurons. Neuron *70*, 66–81.

Hirokawa, N., and Takeda, S. (1998). Gene targeting studies begin to reveal the function of neurofilament proteins. J. Cell Biol. *143*, 1–4.

Hirokawa, N., and Noda, Y. (2008). Intracellular transport and kinesin superfamily proteins, KIFs: structure, function, and dynamics. Physiol. Rev. *88*, 1089–1118.

Hirokawa, N., Niwa, S., and Tanaka, Y. (2010). Molecular motors in neurons: transport mechanisms and roles in brain function, development, and disease. Neuron *68*, 610–638.

Huang, J.D., Brady, S.T., Richards, B.W., Stenolen, D., Resau, J.H., Copeland, N.G., and Jenkins, N.A. (1999). Direct interaction of microtubule- and actin-based transport motors. Nature *397*, 267–270.

Jacob, T.C., Moss, S.J., and Jurd, R. (2008). GABA(A) receptor trafficking and its role in the dynamic modulation of neuronal inhibition. Nat. Rev. Neurosci. *9*, 331–343.

Joyner, A.L. (1993). Gene Targeting: A Practical Approach (Oxford: Oxford University Press).

Kaech, S., and Banker, G. (2006). Culturing hippocampal neurons. Nat. Protoc. *1*, 2406–2415.

Kanai, Y., Okada, Y., Tanaka, Y., Harada, A., Terada, S., and Hirokawa, N. (2000). KIF5C, a novel neuronal kinesin enriched in motor neurons. J. Neurosci. *20*, 6374–6384.

Kittler, J.T., Wang, J., Connolly, C.N., Vicini, S., Smart, T.G., and Moss, S.J. (2000). Analysis of GABAA receptor assembly in mammalian cell lines and hippocampal neurons using γ 2 subunit green fluorescent protein chimeras. Mol. Cell. Neurosci. *16*, 440–452.

Kittler, J.T., Rostaing, P., Schiavo, G., Fritschy, J.M., Olsen, R., Triller, A., and Moss, S.J. (2001). The subcellular distribution of GABARAP and its ability to interact with NSF suggest a role for this protein in the intracellular transport of GABA(A) receptors. Mol. Cell. Neurosci. *18*, 13–25.

Lariviere, R.C., and Julien, J.P. (2004). Functions of intermediate filaments in neuronal development and disease. J. Neurobiol. *58*, 131–148.

Lawrence, C.J., Dawe, R.K., Christie, K.R., Cleveland, D.W., Dawson, S.C., Endow, S.A., Goldstein, L.S., Goodson, H.V., Hirokawa, N., Howard, J., et al. (2004). A standardized kinesin nomenclature. J. Cell Biol. *167*, 19–22.

Leil, T.A., Chen, Z.W., Chang, C.S., and Olsen, R.W. (2004). GABAA receptor-associated protein traffics GABAA receptors to the plasma membrane in neurons. J. Neurosci. *24*, 11429–11438.

Lo, W.Y., Lagrange, A.H., Hernandez, C.C., Harrison, R., Dell, A., Haslam, S.M., Sheehan, J.H., and Macdonald, R.L. (2010). Glycosylation of β2 subunits regulates GABAA receptor biogenesis and channel gating. J. Biol. Chem. *285*, 31348–31361.

Luscher, B., Fuchs, T., and Kilpatrick, C.L. (2011). GABAA receptor trafficking-mediated plasticity of inhibitory synapses. Neuron *70*, 385–409.

Maas, C., Belgardt, D., Lee, H.K., Heisler, F.F., Lappe-Siefke, C., Magiera, M.M., van Dijk, J., Hausrat, T.J., Janke, C., and Kneussel, M. (2009). Synaptic activation modifies microtubules underlying transport of postsynaptic cargo. Proc. Natl. Acad. Sci. USA *106*, 8731–8736.

Mansuy, V., Boireau, W., Fraichard, A., Schlick, J.L., Jouvenot, M., and Delage-Mourroux, R. (2004). GEC1, a protein related to GABARAP, interacts with tubulin and GABA(A) receptor. Biochem. Biophys. Res. Commun. *325*, 639–648.

Mansuy-Schlick, V., Tolle, F., Delage-Mourroux, R., Fraichard, A., Risold, P.Y., and Jouvenot, M. (2006). Specific distribution of gabarap, gec1/gabarap Like 1, gate16/gabarap Like 2, lc3 messenger RNAs in rat brain areas by quantitative real-time PCR. Brain Res. *1073-1074*, 83–87.

Marsden, K.C., Beattie, J.B., Friedenthal, J., and Carroll, R.C. (2007). NMDA receptor activation potentiates inhibitory transmission through GABA receptor-associated protein-dependent exocytosis of GABA(A) receptors. J. Neurosci. *27*, 14326–14337.

McCormick, D.A., and Contreras, D. (2001). On the cellular and network bases of epileptic seizures. Annu. Rev. Physiol. *63*, 815–846.

Miki, H., Okada, Y., and Hirokawa, N. (2005). Analysis of the kinesin superfamily: insights into structure and function. Trends Cell Biol. *15*, 467–476.

Musumeci, O., Bassi, M.T., Mazzeo, A., Grandis, M., Crimella, C., Martinuzzi, A., and Toscano, A. (2011). A novel mutation in KIF5A gene causing hereditary spastic paraplegia with axonal neuropathy. Neurol. Sci. *32*, 665–668.

Nakajima, K., Takei, Y., Tanaka, Y., Nakagawa, T., Nakata, T., Noda, Y., Setou, M., and Hirokawa, N. (2002). Molecular motor KIF1C is not essential for mouse survival and motor-dependent retrograde Golgi apparatus-to-endoplasmic reticulum transport. Mol. Cell. Biol. *22*, 866–873.

Nakata, T., and Hirokawa, N. (1995). Point mutation of adenosine triphosphate-binding motif generated rigor kinesin that selectively blocks anterograde lysosome membrane transport. J. Cell Biol. *131*, 1039–1053.

O'Sullivan, G.A., Kneussel, M., Elazar, Z., and Betz, H. (2005). GABARAP is not essential for GABA receptor targeting to the synapse. Eur. J. Neurosci. *22*, 2644–2648.

Otnes, R.K. (1978). Applied Time Series Analysis (New York: Wiley).

Porjesz, B., Almasy, L., Edenberg, H.J., Wang, K., Chorlian, D.B., Foroud, T., Goate, A., Rice, J.P., O'Connor, S.J., Rohrbaugh, J., et al. (2002). Linkage disequilibrium between the beta frequency of the human EEG and a GABAA receptor gene locus. Proc. Natl. Acad. Sci. USA *99*, 3729–3733.

Reid, E., Kloos, M., Ashley-Koch, A., Hughes, L., Bevan, S., Svenson, I.K., Graham, F.L., Gaskell, P.C., Dearlove, A., Pericak-Vance, M.A., et al. (2002). A kinesin heavy chain (KIF5A) mutation in hereditary spastic paraplegia (SPG10). Am. J. Hum. Genet. *71*, 1189–1194.

Rudolph, U., and Möhler, H. (2004). Analysis of GABAA receptor function and dissection of the pharmacology of benzodiazepines and general anesthetics through mouse genetics. Annu. Rev. Pharmacol. Toxicol. *44*, 475–498.

Sakai, K., and Miyazaki, J. (1997). A transgenic mouse line that retains Cre recombinase activity in mature oocytes irrespective of the cre transgene transmission. Biochem. Biophys. Res. Commun. *237*, 318–324.

Schliwa, M. (2002). Molecular Motors (Winheim, Germany: Wiley-VCH).

Setou, M., Nakagawa, T., Seog, D.H., and Hirokawa, N. (2000). Kinesin superfamily motor protein KIF17 and mLin-10 in NMDA receptor-containing vesicle transport. Science *288*, 1796–1802.

Standley, S., Tocco, G., Wagle, N., and Baudry, M. (1998). High- and low-affinity α-[3H]amino-3-hydroxy-5-methylisoxazole-4-propionic acid ([3H]AMPA) binding sites represent immature and mature forms of AMPA receptors and are composed of differentially glycosylated subunits. J. Neurochem. *70*, 2434–2445.

Takayama, C., and Inoue, Y. (2003). Normal formation of the postsynaptic elements of GABAergic synapses in the reeler cerebellum. Brain Res. Dev. Brain Res. *145*, 197–211.

Tanaka, M., Olsen, R.W., Medina, M.T., Schwartz, E., Alonso, M.E., Duron, R.M., Castro-Ortega, R., Martinez-Juarez, I.E., Pascual-Castroviejo, I., Machado-Salas, J., et al. (2008). Hyperglycosylation and reduced GABA currents of mutated GABRB3 polypeptide in remitting childhood absence epilepsy. Am. J. Hum. Genet. *82*, 1249–1261.

Tanaka, Y., Kanai, Y., Okada, Y., Nonaka, S., Takeda, S., Harada, A., and Hirokawa, N. (1998). Targeted disruption of mouse conventional kinesin heavy chain, *kif5B*, results in abnormal perinuclear clustering of mitochondria. Cell *93*, 1147–1158.

Taniguchi, M., Sanbo, M., Watanabe, S., Naruse, I., Mishina, M., and Yagi, T. (1998). Efficient production of Cre-mediated site-directed recombinants through the utilization of the puromycin resistance gene, pac: a transient gene-integration marker for ES cells. Nucleic Acids Res. *26*, 679–680.

Tobler, I., Kopp, C., Deboer, T., and Rudolph, U. (2001). Diazepam-induced changes in sleep: role of the alpha 1 GABA(A) receptor subtype. Proc. Natl. Acad. Sci. USA *98*, 6464–6469.

Tomita, S., Chen, L., Kawasaki, Y., Petralia, R.S., Wenthold, R.J., Nicoll, R.A., and Bredt, D.S. (2003). Functional studies and distribution define a family of transmembrane AMPA receptor regulatory proteins. J. Cell Biol. *161*, 805–816.

Twelvetrees, A.E., Yuen, E.Y., Arancibia-Carcamo, I.L., MacAskill, A.F., Rostaing, P., Lumb, M.J., Humbert, S., Triller, A., Saudou, F., Yan, Z., and Kittler, J.T. (2010). Delivery of GABAARs to synapses is mediated by HAP1-KIF5 and disrupted by mutant huntingtin. Neuron *65*, 53–65.

Wang, H., and Olsen, R.W. (2000). Binding of the GABA(A) receptor-associated protein (GABARAP) to microtubules and microfilaments suggests involvement of the cytoskeleton in GABARAPGABA(A) receptor interaction. J. Neurochem. *75*, 644–655.

Wang, H., Bedford, F.K., Brandon, N.J., Moss, S.J., and Olsen, R.W. (1999). GABA(A)-receptor-associated protein links GABA(A) receptors and the cytoskeleton. Nature *397*, 69–72.

Xia, C.H., Roberts, E.A., Her, L.S., Liu, X., Williams, D.S., Cleveland, D.W., and Goldstein, L.S. (2003). Abnormal neurofilament transport caused by targeted disruption of neuronal kinesin heavy chain KIF5A. J. Cell Biol. *161*, 55–66.

Xu, M., Gu, Y., Barry, J., and Gu, C. (2010). Kinesin I transports tetramerized Kv3 channels through the axon initial segment via direct binding. J. Neurosci. *30*, 15987–16001.

Yin, X., Feng, X., Takei, Y., and Hirokawa, N. (2012). Regulation of NMDA receptor transport: a KIF17-cargo binding/releasing underlies synaptic plasticity and memory in vivo. J. Neurosci. *32*, 5486–5499.

Zhu, Y., Romero, M.I., Ghosh, P., Ye, Z., Charnay, P., Rushing, E.J., Marth, J.D., and Parada, L.F. (2001). Ablation of NF1 function in neurons induces abnormal development of cerebral cortex and reactive gliosis in the brain. Genes Dev. *15*, 859–876.